Article

Volume 14, Issue 3, 2025, 124

https://doi.org/10.33263/LIANBS143.124

# Investigation of Curcumin Analogs by Molecular Docking, MD Simulation and MM-PBSA Calculation as potzential GSK3- $\beta$ Protein Inhibitor to Treat Wounds

Md Shaekh Forid <sup>1</sup>, Miah Roney <sup>2,3</sup>, A. K. M. Moyeenul Huq <sup>4</sup>, Md. Nazim Uddin <sup>5</sup> Mohd Hamzah Bin Mohd Nasir <sup>6,7</sup>, Mohd Fadhlizil Fasihi Mohd Aluwi <sup>2,3</sup>, Muhammad Saupi Azuri <sup>1</sup>, Wan Maznah Wan Ishak <sup>1,\*</sup>

- Faculty of Chemical and Process Engineering Technology, Universiti Malaysia Pahang Al-Sultan Abdullah, Lebuhraya Persiaran Tun Khalil Yaakob, 26300, Gambang, Kuantan, Pahang, Malaysia; foridpharmacy91@gmail.com (M.S.F.); muhammadsaupi97@gmail.com (M.S.A.); wanmaznah@umpsa.edu.my (W.M.W.I.);
- Faculty of Industrial Science and Technology, Universiti Malaysia Pahang Al-Sultan Abdullah, Lebuhraya Persiaran Tun Khalil Yaakob, 26300, Gambang, Kuantan, Pahang, Malaysia; saroney35@gmail.com (M.R.); fasihi@umpsa.edu.my (M.F.F.M.A.);
- Bio Aromatic Research Centre, Universiti Malaysia Pahang Al-Sultan Abdullah, Lebuhraya Persiaran Tun Khalil Yaakob, 26300, Gambang, Kuantan, Pahang, Malaysia
- <sup>4</sup> Centre for Drug and Herbal Development, Faculty of Pharmacy, Universiti Kebangsaan Malaysia, Jalan Raja Muda Abdul Aziz, Kuala Lumpur 50300, Malaysia; huq\_pharmacy@hotmail.com (AKM.M.H.);
- Institute of Food Science and Technology, Bangladesh Council of Scientific and Industrial Research, Dhaka, Bangladesh; nazimbio@yahoo.com (N.U.);
- Department of Biotechnology, Kulliyyah of Science, International Islamic University of Malaysia (IIUM) Kuantan Campus, Jalan Sultan Ahmad Shah, Bandar Indera Mahkota, 25200 Kuantan, Pahang Darul Makmur, Malaysia; hamzahn@iium.edu.my (M.H.M.N.);
- Research Unit for Bioinformatics and Computational Biology (RUBIC), Kulliyyah of Science, International Islamic University Malaysia, Bandar Indera Mahkota, 25200 Kuantan, Pahang, Malaysia.
- \* Correspondence: wanmaznah@umpsa.edu.my (W.M.W.I.);

### Received: 26.11.2023; Accepted: 7.07.2024; Published: 6.09.2025

**Abstract:** Wound healing is associated with many proteins, among them GSK3-β, which is crucial for cutaneous wound healing. However, no particular treatment option is available to target this protein. Therefore, researchers are actively involved in the urgent development of new wound healing agents that are more effective against the GSK3-β protein. This study aims to identify and forecast potential curcumin analogs to inhibit GSK3-β protein function using an *in-silico* approach. A series of computational approaches, such as ADMET, molecular docking, molecular dynamics simulation, and MM-PBSA. Eight curcumin analogs were identified using the Swiss similarity score. Then, four potential compounds were screened using Druglikeness and ADMET-based assay. Consequently, molecular docking results showed that CHEBI3962 (-40.9219 kcal/mol) and CHEBI65737 (-35.5336 kcal/mol) bound with the lowest interaction energy compared to the co-crystalized ligand (-29.1169 kcal/mol). Furthermore, molecular dynamics simulation revealed that CHEBI65737 is more stable at the active site of GSK3-β. Additionally, MM-PBSA results confirmed that CHEBI65737 (-21.51±4.24 kcal/mol) has the highest binding affinity compared to CHEBI3962 (-15.01±3.99 kcal/mol) and the co-crystalized ligand (-17.49±3.70 kcal/mol). Hence, curcumin analogue CHEBI65737 presents as a promising candidate for further investigation and development as a GSK3-β inhibitor.

# **Keywords:** wound healing; curcumin analogs; GSK3-β protein; molecular docking; MD simulation; MM-PBSA.

© 2025 by the authors. This article is an open-access article distributed under the terms and conditions of the Creative Commons Attribution (CC BY) license (https://creativecommons.org/licenses/by/4.0/), which permits unrestricted use, distribution, and reproduction in any medium, provided the original work is properly cited. The authors retain copyright of

their work, and no permission is required from the authors or the publisher to reuse or distribute this article, as long as proper attribution is given to the original source.

#### 1. Introduction

Wound healing is a complex biological process involving various cellular and molecular mechanisms such as cellular infiltration, inflammation, and proliferation that arise during wound healing and lead to the formation of mature scar tissue and new cell matrices and tissue remodeling [1,2]. These processes are tightly regulated by various growth factors, cytokines, and signaling molecules [3,4]. Glycogen synthase kinase-3 beta (GSK3-β) plays a significant role in wound healing processes by modulating various cellular events crucial for tissue repair and fibrogenesis [5,6]. Studies have shown that GSK3-β influences wound closure, collagen production, cell apoptosis, alpha-SMA expression, and myofibroblast formation during wound healing [6]. Notably, fibroblast-specific deletion of GSK3-β in mice has been linked to accelerated wound closure, increased fibrogenesis, and excessive scarring, highlighting the pivotal role of GSK3-β in regulating these processes [7,8]. Researchers demonstrated that inhibition of GSK3-\beta promotes cell migration and proliferation, leading to faster wound closure [4,9]. Alternatively, the suppression of GSK-3β impacts epithelial differentiation during wound healing [10]. Furthermore, researchers also highlighted that the activation of GSK3-β has been associated with delayed wound healing and impaired tissue regeneration in various experimental models [11]. Researchers claim that GSK-3β is actively involved in angiogenesis, which has a crucial impact on the progress of diabetic wound healing [12]. Challenges in targeting GSK3-β for wound treatment lie in the intricate balance required for optimal wound healing. While GSK3-β inhibition can enhance wound repair by promoting cell proliferation and reducing apoptosis, excessive inhibition can lead to abnormal tissue repair, fibrosis, and scarring. Currently, no approved treatments that specifically target GSK-3β for wound healing. Therefore, screening and assessing the effects of various wound-healing drug candidates targeting GSK3-β as a potential therapeutic target for developing novel woundhealing drugs is important.

Natural products have long been used for their wound-healing properties, and some products contain various bioactive compounds that can promote tissue regeneration and reduce inflammation. Some examples of natural products with wound-healing properties include aloe vera, honey, turmeric, and tea tree oil. These substances have been found to accelerate the healing process, enhance collagen production, and prevent wound infection [13-16]. Natural products often have fewer side effects than synthetic alternatives, making them a preferred choice for many individuals seeking effective wound care solutions. Among several natural compounds, curcumin, a polyphenolic substance derived from Curcuma longa, has exhibited notable beneficial effects on human physiology [16]. Numerous investigations have underscored curcumin's efficacy as a potent agent possessing anticancer, anti-inflammatory, antibacterial, antiviral, antifungal, and wound healing attributes [16-19]. Curcumin analog is a compound that shares structural similarities with curcumin [20]. An in vitro study claimed the curcumin analog is a potential α-glucosidase inhibitor [21]. Furthermore, the research highlighted the potential anti-inflammatory and antibacterial properties of EF24 curcumin analogs through the inhibition of the HIF-1a protein [22]. Noteworthy findings from in vivo and in vitro studies indicated the capability of curcumin analogs to impede the PfATP6 protein in malaria [23]. Computational analysis identified six curcumin analogs as potential ALK5 inhibitors [24]. Recent investigations have spotlighted the curcumin analog DB11672 as a prospective inhibitor of dengue NS2B/NS3 protease [20]. Despite existing research, the exploration of curcumin analogs targeting GSK3- $\beta$  remains limited. Therefore, this study aims to evaluate the curcumin analog as a potential inhibitor of GSK3- $\beta$ .

A compound structurally similar to the query molecules, curcumin, was identified using the web-based tool SwissSimilarity, which provides a user-friendly interface for ligand-based virtual screening of chemical libraries [25]. The available compound libraries, including licensed medications, recognized bioactive compounds, commercially accessible compounds, and synthetically accessible compounds, can be screened using the SwissSimilarity tool [26]. A publicly available database that includes more than 12,000 molecular entities, groups, and classes is now represented by CHEBI [27,28]. This study used Chemical Entities of Biological Interest (CHEBI) libraries and pharmacophore-based screening to screen the curcumin-like bioactive molecules (Figure 1) for wound healing studies targeting the GSK3- $\beta$  protein. Thus, eight compounds were screened using a similarity score (1.000-0.900) from the ChEBI database using pharmacophore-based screening for further studies. Consequently, an ADMET, physicochemical properties, and drug-likeness study was conducted to screen the molecules. Discovery Studio (DS.3) was used for the molecular docking of the selected molecules. Finally, the protein-ligand binding interaction behavior of the lead compound was confirmed through GROMACS for 100 ns duration, and MM-PBSA was performed to evaluate the protein-ligand binding free energy and stability. The current study aims to evaluate the GSK3- $\beta$  inhibitory potential of curcumin and its analogs through their interaction at the GSK-3β active site.

Figure 1. Structure of curcumin and curcumin analog molecules (SwissSimilarity score:1.00 to 0.900)

#### 2. Materials and Methods

#### 2.1. Selection and preparation of ligands.

SwissSimilarity, available at http://www.swisssimilarity.ch, is an online tool offering a user-friendly interface for ligand-based virtual screening of chemical libraries. It provides access to various compound libraries, such as approved drugs, bioactive molecules, commercially available compounds, and synthetically accessible compounds. By utilizing diverse 2D and 3D molecular fingerprints, SwissSimilarity enables the calculation of molecular similarity in different digital formats, facilitating the identification of compounds similar to a query molecule [26]. Curcumin and its closely related curcumin analogs were chosen for this study. The curcumin simile notion obtained from the **PubChem** ((https://pubchem.ncbi.nlm.nih.gov/) database was **SwissSimilarity** pasted into the (http://www. swisssimilarity.ch/), an online program to screen structurally similar curcumin

analogs molecules from Chemical Entities of Biological Interest (ChEBI) database through pharmacophore-based screening [26]. Eight molecules of curcumin analogs with a Swiss similarity score in a range between 1.000 and 0.900 were selected (Figure 2).

# 2.2. Preparation of the structure of ligands and protein.

The 2D structure of curcumin and its analogs was created using the ChemDraw program. The curcumin (CHEBI3966) and eight analogs included CHEBI67263 (dihydroxybergamottin), CHEBI176651 (oxydipropyldibenzoate), CHEBI65737 (demethoxycurcumin), CHEBI176657 (kobusin), CHEBI176667 (glycerin), CHEBI176637 (xanthohumol C), CHEBI5352 (gingerenone A), and CHEBI70703 (dentatin) utilized for further *in-silico* study. Meanwhile, the GSK3-β protein was chosen from the literature and downloaded from the RCSB protein data bank with the PDB ID 5K5N [6].

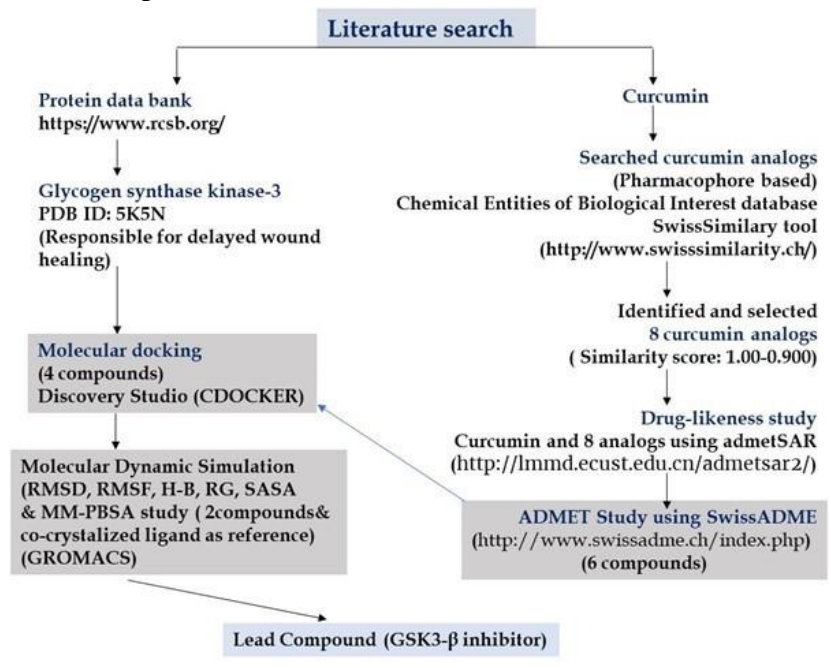


Figure 2. Research flow diagram of this study.

## 2.3. Evaluation of physicochemical properties and drug-likeness study.

The physicochemical characteristics and applicability of all the selected compounds as drug candidates were evaluated based on Lipinski's rule of five using the SwissADME (http://www.swissadme.ch). The six factors assessed included molecular weight, topological polar surface area, molar refractivity, hydrogen bond acceptor, hydrogen bond donor, and the number of rotatable bonds according to Lipinski's rule. The drug-likeness study was determined using the bioavailability score of a compound and the threshold values of Lipinski, Ghose, Egan, Veber, and Muegge.

# 2.4. Evaluation of ADMET properties.

The ADMET assay used the admetSAR (http://lmmd.ecust.edu.cn/admetsar2) prediction web-based tool. The AdmetSAR methodology is a widely used approach for predicting and evaluating the compounds' absorption, distribution, metabolism, excretion, and toxicity properties. It combines various computational models and algorithms to provide comprehensive information on compounds' pharmacokinetic and toxicological behavior. Blood-brain barrier (BBB) penetration, human intestinal absorption (HIA), caco-2

permeability, respiratory toxicity, p-gp substrate, p-gp inhibitor, human ether-a-go-go-related gene (hERG) inhibition, AMES mutagenesis, carcinogens toxicity, and LogS values were obtained by using the admetSAR tool, and values are evaluated.

## 2.5. Molecular docking study.

The computer-aided docking studies were carried out to evaluate the binding location and affinity and determine the interaction between the protein and ligand. Additionally, this approach was used to visualize the receptor-ligand interactions in detail, which allowed for a comprehensive understanding of the molecular interactions between the ligands and the GSK3- $\beta$  protein [6]. Additionally, it provided valuable insights into potential therapeutic targets for developing wound healing potential medicine [29]. The crystal structure suitable for GSK3-β was downloaded from the Protein Data Bank (https://www.rcsb.org/). The molecular docking was carried out using the crystal structure of GSK3-β (PDB ID: 5K5N; Resolution: 2.20 Å), and selected compounds were docked using Discovery Studio 3.1 (DS31.1) [30]. The water molecules and salt ions were removed from the protein by using DS3.1, and hydrogen atoms or the "Prepare Protein" protocol were added to the needed loops. Consequently, protein was minimized, and clean geometry was applied. The rigid docking was used to predict the proteinligand interaction using the CDOCKER protocol. The CDOCKER used the CHARMm force field in DS3.1 to develop a grid box by the input of PDBQT files of protein in DS3.1. The grid box consisted of 11.45 Å, 14.04 Å, and 16.85 Å around the active region, and the grid spacing was 22.87 Å while other parameters were set as default. The binding energy was determined in kcal/mol, where a lower value indicated interactions between the protein and the protein [31]. The 2D interaction forms of the docked complex were used to observe the amino acids present in the protein-ligand binding site. The best two compounds were selected by comparing them with the reference compound (co-crystallized ligand) for a molecular dynamics simulation study and binding free energy calculations to further confirm the selected complex's stability.

# 2.6. Molecular dynamic simulation and MM-PBSA.

Following the docking studies, CHEBI3962 and CHEBI65737 and co-crystalized ligand PF-04802367 were subjected to MD simulation studies for the evaluation of their binding efficacy and to illustrate the effect of compounds binding on the internal dynamics of GSK3-\(\theta\) protein. The MD simulations were performed using the GROMACS (Version 2023.2) molecular dynamics software package, with a CHARMM27 force field for all complexes. The protein and ligand topology were generated using the CHARMM27 force field and TIP3P water model [32]. A total of 17464 water molecules with randomly added Na+ have been introduced to neutralize the simulation system, which is a dodecahedron box. After performing energy minimization, the system was equilibrated with 300 ps NVT (equal particle number N, volume V, temperature T) and NPT of 300 ps (equal particle number N, pressure P, temperature T) followed by MD simulation at 310 K, 1 bar, and 0.002 ps timestep. The Particle-Mesh-Ewald (PME) and linear constraint solver (LINCS) algorithms were used to calculate electrostatic interaction and Hydrogen bonds in the system [33]. The Verlet truncation scheme was used to calculate the van der Waals interaction. In this process, the Parinello-Rahman method for the pressure coupling scheme and the modified Berendsen thermostat were used for the temperature coupling scheme [34,35]. The MD simulation was performed for 100 ns

duration, with three times being carried out for each simulation system, and each (protein and complex) trajectories were stored for the entire simulation period. The RMSD, RMSF, radius of gyration (Rg), SASA, and energies were calculated using the GROMACS utility. MM-PBSA analysis was performed to determine the binding energy of selected CHEBI3962, CHEBI65737, and co-crystalized ligand (PF-04802367) with the protein GSK3- $\beta$ . The MM-PBSA calculations were conducted utilizing the g\_mmpbsa tool, which is compatible with the GROMACS software, as detailed by Kumari et al. (2014) [36].

#### 3. Results and Discussion

#### 3.1. Evaluation of physicochemical properties and drug-likeness study

The drug-likeness studies were carried out using **SwissADME** (http://www.swissadme.ch/) server drug scan tools to optimize the druggability of the compounds. Lipinski's rule of five is a widely used guideline in the drug discovery process [37]. This study was used to filter out all of the chosen compounds' physicochemical properties, such as molecular weight, lipophilicity, hydrogen bond donors, and hydrogen bond acceptors, to determine their potential as drug candidates. The six parameters that were considered were molecular weight, topological polar surface area, molar refractivity, hydrogen bond acceptor, hydrogen bond donor, and number of rotatable bonds. The threshold approaches developed by Lipinski, Ghose, Veber, Egan, and Muegge and the compound's bioavailability score were used to find the drug-like compounds [38-41]. The physicochemical properties and drug-likeness of curcumin and eight curcumin analogs were evaluated, and the results are shown in Table 1.

Table 1. Predicted physicochemical and drug-likeness properties of curcumin and curcumin analogs.

| C            | Dhamine shearded arrest and |        |       |     | Drug-likeness |       |       |    |     |    |     |    |       |     |     |    |      |
|--------------|-----------------------------|--------|-------|-----|---------------|-------|-------|----|-----|----|-----|----|-------|-----|-----|----|------|
| Compound     | Physicochemical properties  |        |       |     |               | Lip   | inski | Gł | ose | Eg | an  | Μι | ıegge | Gho | ose |    |      |
| name         | MW                          | M:R:   | TPSA  | H-A | H-D           | N. R. | Pr    | Vi | Pr  | Vi | Pr  | Vi | Pr    | Vi  | Pr  | Vi | B.S  |
| CHEBI3962    | 368.38                      | 102.80 | 93.06 | 6   | 2             | 8     | Yes   | 0  | Yes | 0  | Yes | 0  | Yes   | 0   | Yes | 0  | 0.55 |
| CHEBI67263   | 372.41                      | 102.17 | 93.06 | 10  | 6             | 2     | Yes   | 0  | Yes | 0  | Yes | 0  | Yes   | 0   | Yes | 0  | 0.55 |
| CHEBI176651  | 342.39                      | 95.67  | 83.83 | 9   | 5             | 2     | Yes   | 0  | Yes | 0  | Yes | 0  | Yes   | 0   | Yes | 0  | 0.55 |
| CHEBI65737   | 338.35                      | 96.31  | 83.83 | 7   | 5             | 2     | Yes   | 0  | Yes | 0  | Yes | 0  | Yes   | 0   | Yes | 0  | 0.55 |
| CHEBI176657  | 370.40                      | 102.4  | 93.06 | 9   | 6             | 2     | Yes   | 0  | Yes | 0  | Yes | 0  | Yes   | 0   | Yes | 0  | 0.55 |
| CHEBI:176667 | 382.41                      | 107.27 | 82.06 | 9   | 6             | 1     | Yes   | 0  | Yes | 0  | Yes | 0  | Yes   | 0   | Yes | 0  | 0.55 |
| CHEBI176637  | 352.38                      | 102.13 | 75.99 | 7   | 5             | 2     | Yes   | 0  | Yes | 0  | Yes | 0  | Yes   | 0   | Yes | 0  | 0.55 |
| CHEBI5352    | 356.41                      | 101.49 | 75.99 | 9   | 5             | 2     | Yes   | 0  | Yes | 0  | Yes | 0  | Yes   | 0   | Yes | 0  | 0.55 |
| CHEBI70703   | 326.39                      | 95.00  | 66.76 | 8   | 4             | 2     | Yes   | 0  | Yes | 0  | Yes | 0  | Yes   | 0   | Yes | 0  | 0.55 |

Molecular weight: MW; Molar refractivity: M.R; Topological polar surface area: TPSA; Num. hydrogen bond acceptor: H-A; Num. hydrogen bond donor: H-D; Num. rotatable bonds: N. R; Pr: Prediction; Vi: Violation.

Curcumin and six other compounds among them successfully passed each assessment in the drug-likeness investigations without failing any of them, including CHEBI3962, CHEBI176651, CHEBI65737, CHEBI176637, CHEBI5352, CHEBI176653, CHEBI70703. From Table 1, all the compounds showed molecular weight values ranging from 326.39 to 382.41, not above 500, and the molar refractivity of the measured compounds ranged from 95.00 to 102.80, which are less than 130, as well as the TPSA values ranging from 66.76 to 93.06Å2. Consequently, the compound number of hydrogen bond acceptors (H-A) is 6–10, which complies with the reference value (less than 10). On the other hand, the number of hydrogen bond donors of the compounds CHEBI 3962, CHEBI 176651, CHEBI 65737, CHEBI176637, CHEBI5352, CHEBI176653, CHEBI70703 ranged from 2-5, which complied with the reference value (not more than 5). However, the number of hydrogen bond donors of the compounds CHEBI 67263, CHEBI176657, CHEBI67262, and CHEBI176667 was 6,

which did not comply with the reference value. A molecule's number of rotatable bonds is essential for conformational changes and, eventually, receptor or channel interaction. The results showed that all the compounds showed fewer rotatable bonds ranging from 1-8, which follows the accepted range value. The six compounds that effectively achieved the abovementioned criteria were expected and considered potential lead compounds with good druggability and thus selected for the ADMET-based study.

#### 3.2. Evaluation of ADMET study.

The results shown in Table 2 provide a comprehensive overview of the ADMET properties of the examined curcumin and curcumin analogs. The AdmetSAR software efficiently analyzed various factors such as absorption, distribution, metabolism, excretion, and toxicity to evaluate their potential effects.

Table 2. Predicted ADMET profile of curcumin and curcumin analogs.

| ADMET                     | CHEBI3962 |       | CHEBI176651 |       | CHEBI65737 |       | CHEBI176637 |       | CHEBI5352 |       | CHEBI70703 |       |
|---------------------------|-----------|-------|-------------|-------|------------|-------|-------------|-------|-----------|-------|------------|-------|
|                           | P         | R     | P           | R     | P          | R     | P           | R     | P         | R     | P          | R     |
| HIA                       | +         | 0.980 | +           | 0.968 | +          | 0.981 | +           | 0.990 | +         | 0.986 | +          | 0.987 |
| BBB                       | -         | 0.625 | -           | 0.775 | -          | 0.675 | -           | 0.700 | -         | 0.650 | -          | 0.675 |
| Caco-2                    | -         | 0.765 | -           | 0.656 | -          | 0.788 | -           | 0.596 | -         | 0.589 | -          | 0.653 |
| P-gp substrate            | -         | 0.936 | -           | 0.629 | -          | 0.887 | -           | 0.952 | -         | 0.881 | -          | 0.776 |
| P-gp Inhibitor            | +         | 0.596 | -           | 0.644 | -          | 0.726 | +           | 0.634 | +         | 0.660 | -          | 0.590 |
| Respiratory toxicity      | No        | 0.822 | No          | 0.566 | No         | 0.833 | No          | 0.900 | No        | 0.533 | No         | 0.577 |
| Hepatotoxicity            | No        | 0.919 | No          | 0.775 | No         | 0.919 | No          | 0.755 | No        | 0.862 | No         | 0.825 |
| Carcinogen                | No        | 0.789 | No          | 0.799 | No         | 0.789 | No          | 0.764 | No        | 0.792 | No         | 0.792 |
| Biodegradation            | -         | 0.800 | -           | 0.800 | -          | 0.850 | -           | 0.875 | -         | 0.925 | -          | 0.900 |
| Acute oral toxicity       | III       | 0.634 | III         | 0.734 | III        | 0.625 | III         | 0.665 | III       | 0.697 | III        | 0.626 |
| Aqueous solubility (logS) |           | -3.36 |             | -3.32 |            | -3.08 |             | -3.82 |           | -3.89 |            | -3.7  |

P: Probability; R: Results; Blood-brain barrier: BBB; Human intestinal absorption: HIA; Cancer coli-2: Caco-2; P-glycoprotein: P-gp.

The findings showed that all the compounds can pass through the intestine, ranging from 0.968 to 0.990. Similarly, all compounds can cross the blood-brain barrier and enter the brain. This is crucial in understanding how these compounds can affect brain function and behavior. All the compounds and reference compounds showed negative results for the P-gp substrate, which indicated that the tested compound is not a substrate for P-glycoprotein (pgp). This suggests that the compound is unlikely to be actively transported out of cells by Pglycoprotein, which may affect its pharmacokinetic properties and potential drug-drug interactions. Additionally, compound CHEBI3962 and tested compounds CHEBI176637 and CHEBI5352 showed a likelihood score of 0.596 and 0.634, 0.660, respectively, which are Pglycoprotein inhibitors, while compound CHEBI176651, CHEBI65737 and CHEBI70703 did not block the action of p-glycoprotein. The positive results for P-glycoprotein inhibitors are promising because this protein plays a crucial role in drug resistance [42]. This inhibition increases drug efficacy and improves treatment outcomes, particularly in cases where Pglycoprotein is overexpressed. Additionally, these positive results highlight the potential of pglycoprotein inhibitors as a promising strategy to overcome multidrug resistance in various diseases, including cancer [43]. Respiratory toxicity of compounds refers to the harmful effects on the respiratory system. This can include irritation, inflammation, lung and airway damage

[44]. All the tested compounds are free from respiratory toxicity. Hepatotoxicity refers to the ability of a compound to cause damage or injury to the liver [45]. This can occur due to the compound's direct toxic effects on liver cells or interference with normal liver function. On the other hand, carcinogenicity refers to the ability of a compound to cause cancer [46]. It is essential to assess both hepatotoxicity and carcinogenicity when evaluating the safety profile of a compound, as these adverse effects can have severe implications for human health. The results demonstrated that all the compounds are free from hepatotoxicity and carcinogenicity, indicating that they are safe for use (Figure 3). A compound's log S solubility results provide valuable information about its ability to dissolve. This data is often used in drug discovery and formulation processes to assess the compound's bioavailability and potential for oral administration. The acute oral toxicity results showed that all the substates are harmless. The aqueous solubility (logS) results ranged from -3.08 to 3.89, demonstrating that all the compounds have good solubility. Thus, it can be concluded that all the compounds have good potential for use as medicine.

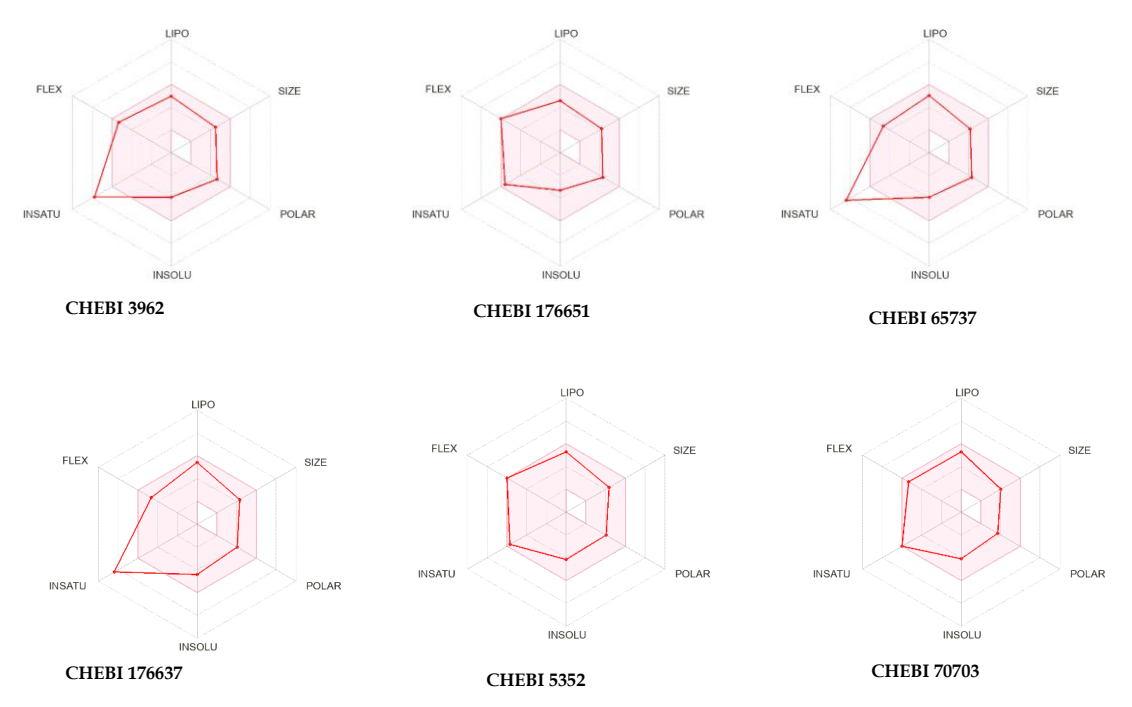


**Figure 3.** Prediction of the physicochemical characteristics of the curcumin analogs. (Lipophilicity: LIPO; Insolubility: INSOLU; Insaturation: INSATU; Flexibility: FLEX; Polarity: POLAR). For oral bioavailability, the colored zone is the ideal physicochemical region.

Lipophilicity and solubility are two essential properties that determine the behavior of a substance in different environments [47]. Lipophilicity refers to the ability of a compound to dissolve in lipids or fats, while solubility is the ability of a substance to dissolve in a given solvent. These properties play a crucial role in drug development, as lipophilic compounds tend to have better absorption and distribution in the body. At the same time, solubility determines how easily a drug can be formulated into various dosage forms of the compound [48]. As shown in Figure 3, all the compounds demonstrated the expected lipophilicity and solubility.

#### 3.3. Molecular docking study.

Based on the ADMET screening, four compounds were selected and subjected to molecular docking against GSK3- $\beta$ . GSK3- $\beta$  is an important promising target for the treatment of wound healing [9,49,50]. Additionally, GSK3- $\beta$  plays a significant role in various cellular

processes, making it an attractive target for drug development beyond wound healing treatments [51]. Understanding these compounds' binding mechanisms and affinities within GSK3- $\beta$ 's active site is essential for advancing effective wound healing therapies. This study employed molecular docking to investigate the binding mechanisms and affinities of the compounds within GSK3- $\beta$ 's active site. The calculated binding energies (kcal/mol) and associated amino acid residues are detailed in Table 3.

| <b>Table 3.</b> The binding energy and | bound amino acids of com | pounds with the wound | healing target GSK3-β. |
|--|--------------------------|-----------------------|------------------------|
|  |                          |                       |                        |

| Compound name                              | CDOCKER<br>interaction energy | Bound amino acids   |  |  |  |  |
|--|-------------------------------|---|--|--|--|--|
| CHEBI3962<br>(Curcumin)                    | -40.9219                      | LYS 183, ARG220, GLN185 (Conventional hydrogen bond); SER219 (Van der Waals); ASP181, SER203 (Carbon hydrogen bond); CYS 218 (Amide Pi- Stacked Bond) |  |  |  |  |
| CHEBI176651                                | -33.6905                      | LYS 183, PTR216 and SER66 (Conventional hydrogen bond)  |  |  |  |  |
| CHEBI65737                                 | -35.5336                      | SER203, CYS218, PTR216, TYR 221 (Conventional hydrogen bond);<br>SER219 (Carbon hydrogen bond); ARG220 (Pi-Alkyl)                                     |  |  |  |  |
| CHEBI70703                                 | -34.6742                      | SER219, LYS 183, CYS218, SER203 (Conventional hydrogen bond)  |  |  |  |  |
| Co-crystallized<br>ligand<br>(PF-04802367) | -29.1169                      | LYS 183, SER219 (Conventional hydrogen bond); PTR216 (Carbon hydrogen bond); ARG220 (Pi-Cation); ARG220 (Pi-Alkyl)                                    |  |  |  |  |

Furthermore, the interactions of bioactive and reference compounds with GSK3-β were visualized using the BIOVIA Discovery Studio visualizer tool, as depicted in Figure 4.

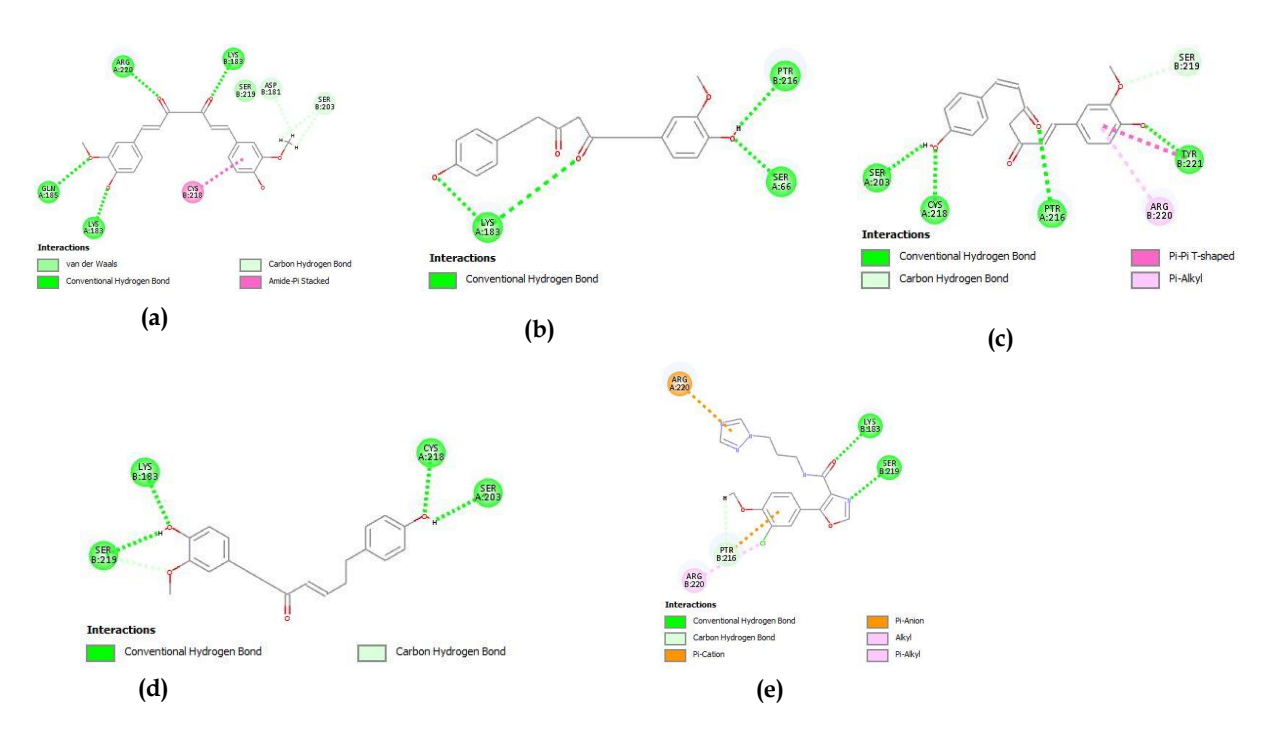


**Figure 4.** Molecular docking interaction analysis of (a) CHEBI3962; (b) CHEBI176651; (c) CHEBI65737; (d) CHEBI70703; (e) PF-04802367 (co-crystallized ligand) with GSK3-β (5K5N).

The results revealed that all the tested compounds showed the lowest interaction energy compared to the co-crystallized ligand (reference compound). However, the CHEBI3962 showed the best binding affinity and lowest binding interaction energy -40.9219 kcal/mol by forming a conventional hydrogen bond with LYS 183, ARG220, GLN185, van der Waals interaction with SER219, carbon-hydrogen bond with ASP181, SER203 and amide pi- stacked bond with CYS 218 residues. Consequently, CHEBI176651 formed conventional hydrogen bonds with LYS 183, PTR216, and SER66 residues and interacted with a binding energy of -

33.6905 kcal/mol. Meanwhile, CHEBI65737 has a binding interaction energy of -35.5336 kcal/mol and forms conventional hydrogen bonds with residues at the hinge region, particularly with SER203, CYS218, PTR216, TYR 221, carbon-hydrogen bonds with SER219 and exhibited pi-alkyl bond with ARG220. This specific orientation of CHEBI65737 within the binding site, adopting propeller-like conformations, contributes to its lower interaction energy. Furthermore, CHEBI70703 formed a conventional hydrogen bond with LYS 183 SER219 and exhibited pi-cation, pi-alkyl bonds, and a binding interaction energy of -34.6742 kcal/mol.

Moreover, the co-crystallized ligand (PF-04802367) developed a conventional hydrogen bond with LYS 183, SER219, a carbon-hydrogen bond with PTR216, a pi-cation bond with ARG220 and pi-alkyl with ARG220 residues and an interaction energy of -29.1169kcal/mol. The best binding affinity of GSK3- $\beta$  was exhibited with the CHEBI3962.

In conclusion, Both CHEBI3962 and CHEBI65737 displayed distinct interactions with proteins, establishing a significant number of hydrogen bonds crucial for the stability of the complex. Therefore, the best binding affinity of GSK3- $\beta$  was exhibited with the CHEBI3962 and CHEBI65737 as compared to co-crystal ligands (PF-04802367). Furthermore, GSK3- $\beta$ /CHEBI3962 and GSK3- $\beta$ /CHEBI65737 complexes have been chosen for subsequent investigation using Molecular Dynamics simulations to assess the stability of the complex.

#### 3.4. Molecular dynamic simulation analysis.

The protein-ligand complex and the protein backbone were evaluated using the RMSD plot for their dynamic conformational stability. As shown in Figure 5(a), the RMSD plot revealed that the CHEBI65737-GSK3- $\beta$  and PF-04802367-GSK3- $\beta$  complexes were in equilibrium, and the protein-ligand complexes maintained stability with a low deviation throughout the MD simulation time with RMSD of 0.25 and 0.48nm, respectively. However, the CHEBI3962-GSK3- $\beta$  complex was more stable until 55 ns; after that, a slight deviation was found, which may have been due to binding confirmation change, but the compound still interacted with the residue at the binding pocket.

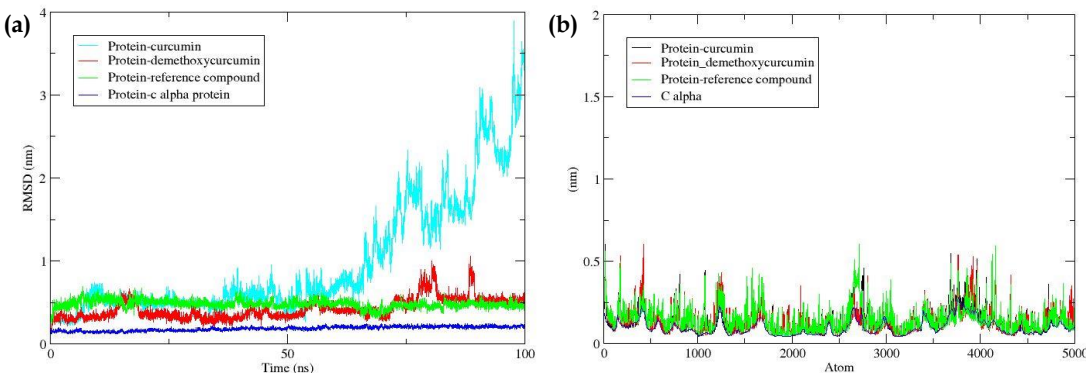


**Figure 5.** Molecular dynamics simulation (a) RMSD plot of compounds and reference; (b) RMSF plot of compound and reference with GSK3-β protein. CHEBI3962- GSK3-β protein complex (blue); CHEBI65737-GSK3-β protein complex (red); PF-04802367-GSK3-β protein (green) complex.

The root mean square fluctuation (RMSF) was further examined to evaluate the residual fluctuations left over after simulating the ligand-bound protein complex. By calculating the RMSF of atomic positions over time, researchers can gain insights into the flexibility and dynamics of molecules. Additionally, RMSF analysis can help identify regions that undergo significant conformational changes, which is valuable for understanding protein folding, ligand binding, and other molecular interactions. Figure 5(b) demonstrates the CHEBI3962-GSK3- $\beta$ , CHEBI65737-GSK3- $\beta$ , and PF-04802367-GSK3- $\beta$  complexes RMSF value. All the

complexes showed RMSF plots that were below 0.5 nm, and the average was below 0.25 nm, which supports that the compounds strongly interacted with the active site of the GSK3- $\beta$  protein. The dynamic stability of the CHEBI3962-GSK3- $\beta$ , CHEBI65737-GSK3- $\beta$ , and PF-04802367-GSK3- $\beta$  complexes was maintained due to the presence of conventional hydrogen bonds between the compounds and the residues of GSK3- $\beta$ .

The radius of gyration (Rg) of all complexes was below 2.2 nm (Figure 6(a)). Consequently, throughout the simulation of CHEBI3962-GSK3 $\beta$ , CHEBI65737-GSK3- $\beta$ , and PF-04802367-GSK3- $\beta$  complexes, the fraction of surface area solvents remained stable at an average area of 160 nm<sup>2</sup> and 180 nm<sup>2</sup> (Figure 6(b)). Overall, the MD simulations and the docking scores of the compounds CHEBI3962 and CHEBI65737 supported the potential inhibitory nature toward the GSK3- $\beta$  protein.

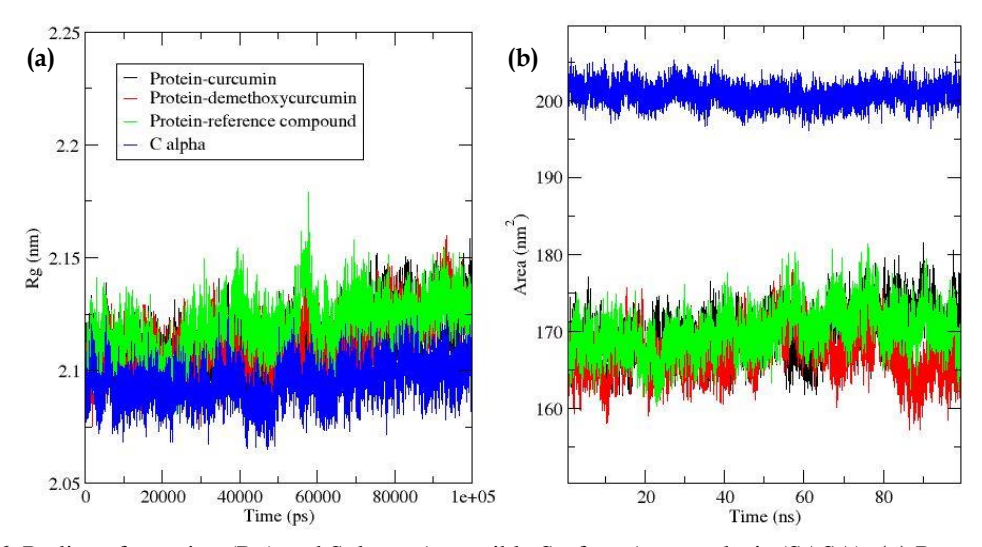


**Figure 6.** Radius of gyration (Rg) and Solvent Accessible Surface Area analysis (SASA). (a) Rg analysis of compound; (b) SASA analysis of compound and reference.

The number of hydrogen bonds formed between compounds and the protein GSK3- $\beta$  is shown in Figure 7. It has been noticed that compounds CHEBI3962 and CHEBI65737 formed six and five hydrogen bonds, respectively, while PF-04802367 formed four hydrogen bonds. These findings demonstrated that CHEBI3962 and CHEBI65737 were bound inside the active site of GSK3- $\beta$  throughout the simulation. The common residues participating in hydrogen bond formations were LYS183, ARG220, GLN185, SER203, CYS218, PTR216, TYR 221 and SER219.

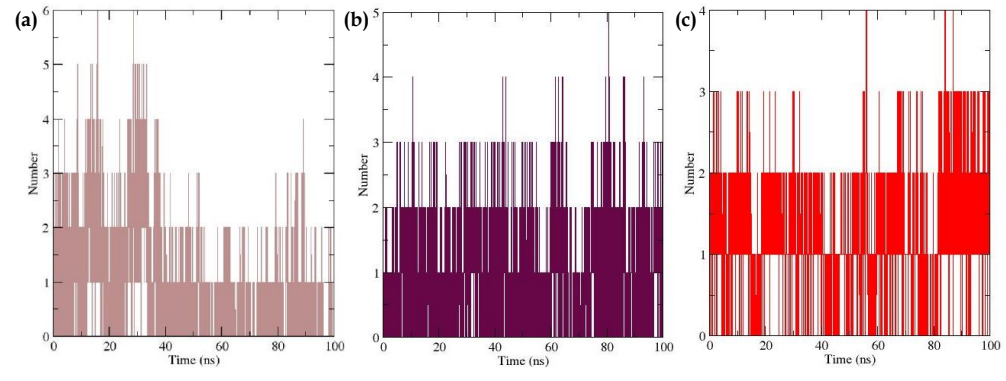


**Figure 7.** Hydrogen bond profile of the GSK3-β with compounds (a) CHEBI3962; (b) CHEBI65737; (c) PF-04802367.

Overall, the RMSD plot indicated consistent stability of the CHEBI65737-GSK3β complex during MD simulation, highlighting dynamic conformational stability. RMSF analysis revealed lower average RMSF values for CHEBI65737-GSK3β compared to the cocrystal ligand, indicating strong interactions with GSK3β active site residues. The Rg of CHEBI65737-GSK3β remained lower than CHEBI65737 and the co-crystal ligand, with stable solvent-accessible surface area fractions, confirming complex stability. Notably, CHEBI65737 formed crucial hydrogen bonds with key GSK3β active site residues (LYS183, ARG220, GLN185, SER203, CYS218, PTR216, TYR221, SER219), underscoring robust binding interactions. Overall, these MD simulation results and favorable docking scores support CHEBI65737's potential as a potent GSK3β inhibitor. The observed stable binding interactions and hydrogen bond formations suggest promising prospects for further exploration of these compounds as GSK3β inhibitors for therapeutic purposes.

#### 3.5. Binding free energy analysis.

The potential affinity of all the compounds with its targeted protein GSK3- $\beta$  was analyzed using the MM-PBSA approach during 100-ns simulation trajectories. The potential energy obtained from MM-PBSA, including van der Waals, electrostatic energy, polar solvation energy, and MM-PBSA binding free energy, are all listed in Table 4. The greater the negative value, the greater the binding affinity towards protein [29,52].

**Table 4.** Binding free energy calculations of selected compounds in GSK3- $\beta$  using MM-PBSA.

| Compounds in complex |             | Van der Waal energy | Electrostatic energy | Polar solvation energy | Binding energy |  |  |
|----------------------|-------------|---------------------|----------------------|------------------------|----------------|--|--|
|                      | with GSK3-β | (kcal/mol)          | (kcal/mol)           | (kcal/mol)             | (kcal/mol)     |  |  |
|                      | CHEBI3962   | -23.26±0.78         | -17.88±3.70          | 26.13±1.25             | -15.01± 3.99   |  |  |
|                      | CHEBI65737  | -32.79±0.13         | -20.40±4.21          | 31.68± 0.40            | -21.51±4.24    |  |  |
|                      | PF-04802367 | -47.76±0.33         | -21.44±6.4           | 48.09±0.18             | -17.49±3.70    |  |  |

From Table 4, it has been shown that demethoxycurcumin formed the most stable complex with GSK3- $\beta$  (-21.51±4.24 kcal/mol), compared to curcumin (-15.01± 3.99 kcal/mol) and PF-04802367 (-17.49±3.70 kcal/mol). It should also be noted that, apart from demethoxycurcumin, both curcumin and PF-04802367 also formed stable bindings. It was also observed that nonpolar interaction energy, i.e., the sum of van der Waal's energy and nonpolar solvation energy, contributes strongly towards the binding of two compounds, reference ligands, and the protein GSK3- $\beta$ , indicating hydrophobic forces favor the formation of the complexes.

#### 4. Discussion

Wound healing is a global health concern worldwide. Several inflammatory cytokines regulate wound healing, such as TNF- $\alpha$ , TGF- $\beta$ , and GSK3- $\beta$  [53]. Studies reported that high levels of GSK3- $\beta$  beta delay the granulation tissue formation and failure of wound closure [8]. Therefore, GSK3- $\beta$ , which has essential roles in regulating cell function, such as proliferation, migration, and matrix synthesis, is a good target for wound healing treatment. Curcumin is a famous traditional herbal medicine with antioxidant, anti-inflammatory, anti-fibrosis, anti-diabetes, and wound healing properties [16]. However, curcumin analogs targeting the GSK3- $\beta$  are still unknown. Therefore, in this study, we aimed to investigate curcumin and its analog targeting inhibition of the GSK3- $\beta$  protein through an *in-silico* approach.

The SwissSimilary tool identified the 8 molecules that have a molecular structure similar to curcumin based on the Swiss similarity score of 1.00- 0.900 (Figure 1). The drug-

likeness study demonstrated that curcumin and its five analogs, CHEBI3962, CHEBI176651, CHEBI65737, CHEBI176637, CHEBI5352, and CHEBI70703, comply with the pharmacokinetics criteria (Table 1). Additionally, these compounds showed expected lipophilicity and solubility (Figure 3). Consequently, the AMDET results show that CHEBI3962, CHEBI176651, CHEBI65737, and CHEBI70703 are suitable for drug development as they passed all the criteria (Table 2). Furthermore, the docking results revealed that all the tested compounds showed the best binding affinity with a lower interaction energy than the co-crystallized ligand (PF-04802367). However, among them, CHEBI3962 and CHEBI65737 binding interaction were -40.9219 kcal/mol and -35.5336 kcal/mol, which are significantly lower than co-crystallized ligand (-29.1169 kcal/mol). Additionally, CHEBI3962 formed a vital hydrogen bond with LYS 183, ARG220, GLN185 while CHEBI65737 formed hydrogen bond with SER203, CYS218, PTR216, TYR221 (Figure 4 and Table 3). Studyreported results indicated that the binding energy between the phenylethanoid glycosides and GSK3-β ranged from -10.2 kcal/mol to a lower value, suggesting a stable interaction between the ligand and the target protein [54]. Thus, these docking results indicate that the CHEBI3962 and CHEBI65737 are bound to the active site of the GSK3-β.

Furthermore, the CHEBI3962 and CHEBI65737 and co-crystalized ligands were evaluated through a 100 ns MD simulation study to confirm the binding behavior of the docking. The molecular dynamic simulation was analyzed to check the stability of the docked compound by evaluating several parameters, including the RMSD, RMSF, Rg, SASA, and Hbond occupancy during simulation events of protein-ligand complexes [55]. The RMSD plot confirmed that the CHEBI65737 and PF-04802367 complex was below 0.25nm while CHEBI3962 showed a low deviation after 55ns (Figure 5 (a)). A study reported that RMSD values below 0.5 nm and 0.05 nm deviation indicate stable interaction of protein-ligand complex, and no conformation change occurred [56]. A similar study reported that the RMSD value of Kaempferol and COVID-19 Mpro was 0.617 nm, which was stable [57]. Another study demonstrated that the RMSD value of a protein-ligand complex with an average of 0.757 nm is stable [58]. Therefore, it can be concluded that compound CHEBI65737 formed stable binding in the active site of GSK3-\beta. The RMSF values of all CHEBI3962, CHEBI65737, and co-crystalized complexes have been calculated and depicted in Figure 5(b). The low RMSF values of amino acid residues define stable and rigid receptors. Our finding demonstrated that CHEBI3962 (0.14±0.11) and CHEBI65737 (0.14±0.08) formed low fluctuation compared to the co-crystalized ligand (0.15±0.07). This suggests that GSK3-β has formed a stable and rigid complex with CHEBI3962 and CHEBI65737.

In contrast, the Rg was calculated on the intrinsic dynamics of GSK3- $\beta$  and ligand complexes (Figure 6 (a)). Rg is the structural folding, stability, and compactness indicator. Our results demonstrated that for the course of the 100 ns MD simulation, the average Rg for all the complexes was 2.11. These findings indicated that all the ligands formed compact and stable complexes with GSK3- $\beta$  compared to the co-crystal ligand. The SASA was found to be lower for CHEBI65737 (167.09±2.90) compared to the CHEBI3962 (169.71±2.87) and co-crystalized ligand (169.98±2.88) (Figure 6 (b)). Researchers reported hydrogen bonds are the main stabilizing interaction factor between two molecules [55]. Our finding revealed that CHEBI65737 and CHEBI3962 formed more stable hydrogen bonds than the co-crystalized ligand at the inhibition site of GSK3- $\beta$  (Figure 7). Likewise, the MM-PBSA assay identified a more accurate binding free energy between GSK3- $\beta$  and selected ligands at the receptor inhibition site. Studies reported that the binding free energy defines the total of non-bonded

interaction energies such as van der Wall, polar solvation, electrostatic, and energy between receptor and ligand throughout the 100 ns MD simulation [55]. According to previous studies, lower binding free energy indicates a better binding between the ligand and receptor [29,52]. Our finding showed that CHEBI65737 was bound in the active site of GSK3- $\beta$  with the lowest interaction energy compared to the co-crystalized ligand (Table 4). Overall, our in-silico results indicate that CHEBI3962 and its analog CHEBI65737 may have the potential to be developed as inhibitors of GSK3- $\beta$  for wound healing applications.

#### 5. Conclusions

The compound similarity analysis was employed to evaluate the potential of curcuminlike compounds as drug candidates, while docking analysis provided insights into their binding affinity towards target proteins. The drug-likeness and ADMET analysis also assessed the compounds' potential for absorption, distribution, metabolism, excretion, and toxicity in the human body. Compared to the co-crystalized ligand, the results showed that CHEBI65737 had the best binding affinity into the GSK3- $\beta$  protein and displayed acceptable physicochemical and pharmacokinetic features. Therefore, the CHEBI65737 compound could potentially be considered for further study as a lead agent for wound healing.

#### **Author Contributions**

All authors have read and agreed to the published version of the manuscript.

#### **Institutional Review Board Statement**

Not applicable.

#### **Informed Consent Statement**

Not applicable.

# **Data Availability Statement**

Data supporting the findings of this study are available upon reasonable request from the corresponding author.

#### **Funding**

The authors are grateful to the Ministry of Higher Education, Malaysia, for providing the funding under the Fundamental Research Grant Scheme (FRGS) No. FRGS/ 1/2021/STG05/UMP/02/6 (University Reference-RDU210133) and Universiti Malaysia Pahang for providing laboratory facilities, as well as additional funding under Postgraduate Research Grants Scheme (PGRS) Grant (University reference-PGRS220353).

# Acknowledgments

The authors thank the Faculty of Chemical and Process Engineering Technology, University Malaysia Pahang Al-Sultan Abdullah, for encouraging us to perform this research.

#### **Conflicts of Interest**

The authors declare no conflict of interest.

#### References

- 1. Wang, G.; Yang, F.; Zhou, W.; Xiao, N.; Luo, M.; Tang, Z. The initiation of oxidative stress and therapeutic strategies in wound healing. *Biomed. Pharmacother.* **2023**, *157*, 114004, https://doi.org/10.1016/j.biopha.2022.114004.
- Singh, K.; Yadav, V.B.; Yadav, U.; Nath, G.; Srivastava, A.; Zamboni, P.; Kerkar, P.; Saxena, P.S.; Singh, A.V. Evaluation of biogenic nanosilver-acticoat for wound healing: A tri-modal in silico, in vitro and in vivo study. *Colloids Surf. A: Physicochem. Eng. Asp.* 2023, 670, 131575, https://doi.org/10.1016/j.colsurfa.2023.131575.
- 3. Xu, X.; Zeng, Y.; Chen, Z.; Yu, Y.; Wang, H.; Lu, X.; Zhao, J.; Wang, S. Chitosan-based multifunctional hydrogel for sequential wound inflammation elimination, infection inhibition, and wound healing. *Int. J. Biol. Macromol.* **2023**, *235*, 123847, https://doi.org/10.1016/j.ijbiomac.2023.123847.
- Konain, K.; Saddique, N.; Samie, M.; Rahman, Z.U.; Farid, S.; Hameed, S.; Mirza, M.R.; Wu, W.; Woo, K.M.; Arany, P.R.; Rahman, S.U. Curcumin-Loaded Nanofibrous Matrix Accelerates Fibroblast Cell Proliferation and Enhances Wound Healing via GSK3-β Inhibition. *J. Compos. Sci.* 2023, 7, 343, https://doi.org/10.3390/jcs7080343.
- 5. Jere, S.W.; Houreld, N.N.; Abrahamse, H. Role of the PI3K/AKT (mTOR and GSK3β) signalling pathway and photobiomodulation in diabetic wound healing. *Cytokine Growth Factor Rev.* **2019**, *50*, 52-59, https://doi.org/10.1016/j.cytogfr.2019.03.001.
- 6. Aksoy, H.; Şekerler, T.; Mert, N.M. In silico investigation of wound healing potential of some compounds in tubers of Asphodelus species with GSK3-β protein. *J. Res. Pharm.* **2021**, 25, 747-754, https://dx.doi.org/10.29228/jrp.65.
- 7. Yan, N.; Xie, F.; Tang, L.-Q.; Wang, D.-F.; Li, X.; Liu, C.; Liu, Z.-P. Synthesis and biological evaluation of thieno[3,2-c]pyrazol-3-amine derivatives as potent glycogen synthase kinase 3β inhibitors for Alzheimer's disease. *Bioinorg. Chem.* **2023**, *138*, 106663, https://doi.org/10.1016/j.bioorg.2023.106663.
- 8. Nehete, M.; De, S.; Degani, M.; Tatke, P. A topical formulation of Anacardium occidentale L. leaves extract enhances wound healing via mediating TNF-α and TGF-β. *Indian J. Exp. Biol.* **2023**, *61*, 424-435, https://doi.org/10.56042/ijeb.v61i06.1926.
- 9. Paramesha, M.; Ramesh, C.K.; Krishna, V.; Kumar Swamy, H.M.; Aditya Rao, S.J.; Hoskerri, J. Effect of dehydroabietylamine in angiogenesis and GSK3-β inhibition during wound healing activity in rats. *Med. Chem. Res.* **2015**, *24*, 295-303, https://doi.org/10.1007/s00044-014-1110-1.
- 10. Chen, R.-F.; Lin, Y.-N.; Liu, K.-F.; Wang, C.-T.; Ramachandran, S.; Wang, C.-J.; Kuo, Y.-R. The Acceleration of Diabetic Wound Healing by Low-Intensity Extracorporeal Shockwave Involves in the GSK-3β Pathway. *Biomedicines* **2021**, *9*, 21, https://doi.org/10.3390/biomedicines9010021.
- 11. Slominski, A.T.; Zmijewski, M.A. Glucocorticoids İnhibit Wound Healing: Novel Mechanism of Action. *J. Investig. Dermatol.* **2017**, *137*, 1012-1014, https://doi.org/10.1016/j.jid.2017.01.024.
- Lei, T.; Gao, Y.; Duan, Y.; Cui, C.; Zhang, L.; Si, M. *Panax notoginseng* saponins improves healing of high glucose-induced wound through the GSK-3β/β-catenin pathway. *Environ. Toxicol.* 2022, 37, 1867-1877, https://doi.org/10.1002/tox.23533.
- 13. Pleeging, C.C.F.; Wagener, F.A.D.T.G.; de Rooster, H.; Cremers, N.A.J. Revolutionizing non-conventional wound healing using honey by simultaneously targeting multiple molecular mechanisms. *Drug Resist. Updates* **2022**, *62*, 100834, https://doi.org/10.1016/j.drup.2022.100834.
- 14. Altinkaynak, C.; Haciosmanoglu, E.; Ekremoglu, M.; Hacioglu, M.; Özdemir, N. Anti-microbial, anti-oxidant and wound healing capabilities of *Aloe vera*-incorporated hybrid nanoflowers. *J. Biosci. Bioeng.* **2023**, *135*, 321-330, https://doi.org/10.1016/j.jbiosc.2023.01.004.
- 15. Hu, K.; Jia, E.; Zhang, Q.; Zheng, W.; Sun, R.; Qian, M.; Tan, Y.; Hu, W. Injectable carboxymethyl chitosan-genipin hydrogels encapsulating tea tree oil for wound healing. *Carbohydr. Polym.* **2023**, *301*, 120348, https://doi.org/10.1016/j.carbpol.2022.120348.
- 16. Sood, A.; Dev, A.; Das, S.S.; Kim, H.J.; Kumar, A.; Thakur, V.K.; Han, S.S. Curcumin-loaded alginate hydrogels for cancer therapy and wound healing applications: A review. *Int. J. Biol. Macromol.* **2023**, *232*, 123283, https://doi.org/10.1016/j.ijbiomac.2023.123283.

- 17. Obeid, M.A.; Alsaadi, M.; Aljabali, A.A. Recent updates in curcumin delivery. *J. Liposome Res.* **2023**, *33*, 53-64, https://doi.org/10.1080/08982104.2022.2086567.
- 18. Gayathri, K.; Bhaskaran, M.; Selvam, C.; Thilagavathi, R. Nano formulation approaches for curcumin delivery- a review. *J. Drug Deliv. Sci. Technol.* **2023**, 82, 104326, https://doi.org/10.1016/j.jddst.2023.104326.
- 19. Pan-On, S.; Dilokthornsakul, P.; Tiyaboonchai, W. Trends in advanced oral drug delivery system for curcumin: A systematic review. *J. Control. Release* **2022**, *348*, 335-345, https://doi.org/10.1016/j.jconrel.2022.05.048.
- 20. Roney, M.; Huq, A.M.; Aluwi, M.F.F.M.; Tajuddin, S.N. *In-silico* Design of Curcumin Analogs as Potential Inhibitors of Dengue Virus NS2B/NS3 Protease. *J. Comput. Biophys. Chem.* **2023**, 22, 645-653, https://doi.org/10.1142/S2737416523500321.
- 21. Dohutia, C.; Chetia, D.; Gogoi, K.; Sarma, K. Design, *in silico* and *in vitro* evaluation of curcumin analogues against *Plasmodium falciparum*. *Exp. Parasitol*. **2017**, *175*, 51-58, https://doi.org/10.1016/j.exppara.2017.02.006.
- 22. Ardiansah, B.; Hardhani, M.R.; Putera, D.D.S.R.; Wukirsari, T.; Cahyana, A.H.; Jia, J.; Khan, M.M. Design, synthesis, and antioxidant evaluation of monocarbonyl curcumin analogues tethered 1,2,3-triazole scaffold. *ase Stud. Chem. Environ. Eng.* **2023**, 8, 100425, https://doi.org/10.1016/j.cscee.2023.100425.
- 23. Du, Z.-y.; Liu, R.-r.; Shao, W.-y.; Mao, X.-p.; Ma, L.; Gu, L.-q.; Huang, Z.-s.; Chan, A.S.C. α-Glucosidase inhibition of natural curcuminoids and curcumin analogs. *Eur. J. Med. Chem.* **2006**, *41*, 213-218, https://doi.org/10.1016/j.ejmech.2005.10.012.
- 24. He, Y.; Li, W.; Hu, G.; Sun, H.; Kong, Q. Bioactivities of EF24, a Novel Curcumin Analog: A Review. *Front. Oncol.* **2018**, *8*, 614, https://doi.org/10.3389/fonc.2018.00614.
- 25. Khudhayer Oglah, M.; Fakri Mustafa, Y. Curcumin analogs: synthesis and biological activities. *Med. Chem. Res.* **2020**, *29*, 479-486, https://doi.org/10.1007/s00044-019-02497-0.
- 26. Bragina, M.E.; Daina, A.; Perez, M.A.S.; Michielin, O.; Zoete, V. The SwissSimilarity 2021 Web Tool: Novel Chemical Libraries and Additional Methods for an Enhanced Ligand-Based Virtual Screening Experience. *Int. J. Mol. Sci.* 2022, 23, 811, https://doi.org/10.3390/ijms23020811.
- 27. Zoete, Vincent, Antoine Daina, Christophe Bovigny, and Olivier Michielin. "SwissSimilarity: a web tool for low to ultra high throughput ligand-based virtual screening. *J. Chem. Inf. Model.* 2016, 56, 8, 1399–1404. https://doi.org/10.1021/acs.jcim.6b00174.
- 28. Degtyarenko, K.; de Matos, P.; Ennis, M.; Hastings, J.; Zbinden, M.; McNaught, A.; Alcántara, R.; Darsow, M.; Guedj, M.; Ashburner, M. ChEBI: a database and ontology for chemical entities of biological interest. *Nucleic Acids Res.* **2008**, *36*, D344-D350, https://doi.org/10.1093/nar/gkm791.
- 29. Rathnayake, S.; Madushanka, A.; Wijegunawardana, N.D.A.; Mylvaganam, H.; Rathnayake, A.; Perera, E.G.; Jayamanna, I.; Chandrasena, P.; Ranaweera, A.; Jayasooriya, P.; Bamunuarachchige, C. *In Silico* Study of 5,7-Dimethoxycoumarin and p-Coumaric Acid in *Carica* papaya Leaves as Dengue Virus Type 2 Protease Inhibitors. *Proceedings* **2021**, *79*, 11, https://doi.org/10.3390/IECBM2020-08820.
- 30. Roney, M.; Huq, A.K.M.M.; Rullah, K.; Hamid, H.A.; Imran, S.; Islam, M.A.; Mohd Aluwi, M.F.F. Virtual Screening-Based Identification of Potent DENV-3 RdRp Protease Inhibitors via In-House Usnic Acid Derivative Database. *J. Comput. Biophys. Chem.* **2021**, 20, 797-814, https://doi.org/10.1142/S2737416521500496.
- 31. Mone, N.S.; Syed, S.; Ravichandiran, P.; Kamble, E.E.; Pardesi, K.R.; Salunke-Gawali, S.; Rai, M.; Vikram Singh, A.; Prasad Dakua, S.; Park, B.-H.; Yoo, D.J.; Satpute, S.K. Synergistic and Additive Effects of Menadione in Combination with Antibiotics on Multidrug-Resistant *Staphylococcus aureus*: Insights from Structure-Function Analysis of Naphthoquinones. *ChemMedChem* **2023**, *18*, e202300328, https://doi.org/10.1002/cmdc.202300328.
- 32. Qais, F.A.; Sarwar, T.; Ahmad, I.; Khan, R.A.; Shahzad, S.A.; Husain, F.M. Glyburide inhibits non-enzymatic glycation of HSA: An approach for the management of AGEs associated diabetic complications. *Int. J. Biol. Macromol.* **2021**, *169*, 143-152, https://doi.org/10.1016/j.ijbiomac.2020.12.096.
- 33. Kenneth, C.; Anugrah, D.S.B.; Julianus, J.; Junedi, S. Molecular insights into the inhibitory potential of anthocyanidins on glucokinase regulatory protein. *PloS one* **2023**, *18*, e0288810, https://doi.org/10.1371/journal.Pone.0288810.
- 34. Essmann, U.; Perera, L.; Berkowitz, M.L.; Darden, T.; Lee, H.; Pedersen, L.G. A smooth particle mesh Ewald method. *J. Chem. Phys.* **1995**, *103*, 8577-8593, https://doi.org/10.1063/1.470117.

- 35. Hess, B.; Bekker, H.; Berendsen, H.J.; Fraaije, J.G.E.M. LINCS: A linear constraint solver for molecular simulations. *J. Comput. Chem.* **1997**, *18*, 1463-1472, https://doi.org/10.1002/(SICI)1096-987X(199709)18:12%3C1463::AID-JCC4%3E3.0.CO;2-H.
- 36. Kumari, R.; Kumar, R.; Lynn, A. *g\_mmpbsa*—A GROMACS Tool for High-Throughput MM-PBSA Calculations. *J. Chem. Inf. Model.* **2014**, *54*, 1951-1962, https://doi.org/10.1021/ci500020m.
- 37. Rai, M.; Singh, A.V.; Paudel, N.; Kanase, A.; Falletta, E.; Kerkar, P.; Heyda, J.; Barghash, R.F.; Pratap Singh, S.; Soos, M. Herbal concoction Unveiled: A computational analysis of phytochemicals' pharmacokinetic and toxicological profiles using novel approach methodologies (NAMs). *Curr. Res. Toxicol.* **2023**, *5*, 100118, https://doi.org/10.1016/j.crtox.2023.100118.
- 38. Ghose, A.K., Viswanadhan, V.N. and Wendoloski, J.J. A knowledge-based approach in designing combinatorial or medicinal chemistry libraries for drug discovery. 1. A qualitative and quantitative characterization of known drug databases. *Journal of combinatorial chemistry* **1999**, 1, 55-68, https://doi.org/10.1021/cc9800071..
- 39. Veber, D.F.; Johnson, S.R.; Cheng, H.-Y.; Smith, B.R.; Ward, K.W.; Kopple, K.D. Molecular Properties That Influence the Oral Bioavailability of Drug Candidates. *J. Med. Chem.* **2002**, *45*, 2615-2623, https://doi.org/10.1021/jm020017n.
- 40. Egan, W.J.; Merz, K.M.; Baldwin, J.J. Prediction of Drug Absorption Using Multivariate Statistics. *J. Med. Chem.* **2000**, *43*, 3867-3877, https://doi.org/10.1021/jm000292e.
- 41. Muegge, I.; Heald, S.L.; Brittelli, D. Simple Selection Criteria for Drug-like Chemical Matter. *J. Med. Chem.* **2001**, *44*, 1841-1846, https://doi.org/10.1021/jm015507e.
- 42. Dong, J.; Yuan, L.; Hu, C.; Cheng, X.D.; Qin, J.-J. Strategies to overcome cancer multidrug resistance (MDR) through targeting P-glycoprotein (ABCB1): an updated review. *Pharmacol. Ther.* **2023**, 249, 108488, https://doi.org/10.1016/j.pharmthera.2023.108488.
- 43. Kang, X.; Wang, J.; Huang, C.-H.; Wibowo, F.S.; Amin, R.; Chen, P.; Li, F. Diethyldithiocarbamate copper nanoparticle overcomes resistance in cancer therapy without inhibiting P-glycoprotein. *Nanomed.: Nanotechnol. Biol. Med.* **2023**, *47*, 102620, https://doi.org/10.1016/j.nano.2022.102620.
- 44. Wong, J.; Magun, B.; Wood, L. Lung inflammation caused by inhaled toxicants: a review. *Int. J. Chronic Obstr. Pulm. Dis.* **2016**, *11*, 1391-1401, https://doi.org/10.2147/COPD.S106009.
- 45. Woolbright, B.L.; Jaeschke, H. Mechanisms of Inflammatory Liver Injury and Drug-Induced Hepatotoxicity. *Curr. Pharmacol. Rep.* **2018**, *4*, 346-357, https://doi.org/10.1007/s40495-018-0147-0.
- 46. Slika, H.; Mansour, H.; Wehbe, N.; Nasser, S.A.; Iratni, R.; Nasrallah, G.; Shaito, A.; Ghaddar, T.; Kobeissy, F.; Eid, A.H. Therapeutic potential of flavonoids in cancer: ROS-mediated mechanisms. *Biomed. Pharmacother.* **2022**, *146*, 112442, https://doi.org/10.1016/j.biopha.2021.112442.
- 47. Paudel, N.; Rai, M.; Adhikari, S.; Thapa, A.; Bharati, S.; Maharjan, B.; Shrestha, R.L.S.; Rav, K.; Singh, A.V. Green Extraction, Phytochemical Profiling, and Biological Evaluation of *Dysphania ambrosioides*: An *In Silico* and *In Vitro* Medicinal Investigation. *J. Herbs Spices Med. Plants* **2024**, *30*, 97-114, https://doi.org/10.1080/10496475.2023.2267467.
- 48. Bendjedid, S.; Benouchenne, D. *In silico* studies for assessing physicochemical, pharmacokinetic and cytotoxicity properties of bioactive molecules identified by LC-MS in *Aloe vera* leaves extracts. *S. Afr. J. Bot.* **2023**, *157*, 75-81, https://doi.org/10.1016/j.sajb.2023.03.052.
- 49. Subbukutti, V.; Sailatha, E.; Gunasekaran, S.; Manibalan, S.; Uma Devi, K.J.; Bhuvaneshwari, K.; Suvedha, R. Evaluation of wound healing active principles in the transdermal patch formulated with crude bio wastes and plant extracts against GSK-3 beta an *in silico* study. *J. Biomol. Struct. Dyn.* **2024**, *42*, 559-570, https://doi.org/10.1080/07391102.2023.2194424.
- 50. Harish, B.G.; Krishna, V.; Santosh Kumar, H.S.; Khadeer Ahamed, B.M.; Sharath, R.; Kumara Swamy, H.M. Wound healing activity and docking of glycogen-synthase-kinase-3-β-protein with isolated triterpenoid lupeol in rats. *Phytomedicine* **2008**, *15*, 763-767, https://doi.org/10.1016/j.phymed.2007.11.017.
- 51. Thapa, R., Gupta, G., Bhat, A. A., Almalki, W. H., Alzarea, S. I., Kazmi, I., ... & Dua, K. A review of Glycogen Synthase Kinase-3 (GSK3) inhibitors for cancers therapies. *Int. J. Biol. Macromol.* 2023, 253,7, 127375, https://doi.org/10.1016/j.ijbiomac.2023.127375.
- 52. Abdi, F.; Movahedi, M.; Alavı Nikje, M.A.; Ghanei, L.; Mirzaie, S. Vitamin D as a modulating agent of metformin and insulin in patients with type 2 diabetes. *J. Res. Pharm.* **2019**, 23, 360-378, https://doi.org/10.12991/jrp.2019.144.

- 53. Ban, E.; Jeong, S.; Park, M.; Kwon, H.; Park, J.; Song, E.J.; Kim, A. Accelerated wound healing in diabetic mice by miRNA-497 and its anti-inflammatory activity. *Biomed. Pharmacother.* **2020**, *121*, 109613, https://doi.org/10.1016/j.biopha.2019.109613.
- 54. Majie, A.; Saha, R.; Sarkar, B. In Silico Study to Evaluate the Inhibitory Activity of a Few Phenylethanoid Glycosides on GSK3-β Protein for Faster Diabetic Wound Healing. *Med. Sci. Forum* **2023**, *21*, 21, https://doi.org/10.3390/ECB2023-14134.
- 55. Singh, A.V.; Kayal, A.; Malik, A.; Maharjan, R.S.; Dietrich, P.; Thissen, A.; Siewert, K.; Curato, C.; Pande, K.; Prahlad, D.; Kulkarni, N.; Laux, P.; Luch, A. Interfacial Water in the SARS Spike Protein: Investigating the Interaction with Human ACE2 Receptor and In Vitro Uptake in A549 Cells. *Langmuir* **2022**, *38*, 7976-7988, https://doi.org/10.1021/acs.langmuir.2c00671.
- 56. Arnittali, M.; Rissanou, A.N.; Harmandaris, V. Structure Of Biomolecules Through Molecular Dynamics Simulations. *Procedia Comput. Sci.* **2019**, *156*, 69-78, https://doi.org/10.1016/j.procs.2019.08.181.
- 57. Majumder, R.; Mandal, M. Screening of plant-based natural compounds as a potential COVID-19 main protease inhibitor: an *in silico* docking and molecular dynamics simulation approach. *J. Biomol. Struct. Dyn.* **2022**, *40*, 696-711, https://doi.org/10.1080/07391102.2020.1817787.
- 58. Nagar, P.R.; Gajjar, N.D.; Dhameliya, T.M. In search of SARS CoV-2 replication inhibitors: virtual screening, molecular dynamics simulations and ADMET analysis. *Journal of Molecular Structure* **2021**, *1246*, 131190, https://doi.org/10.1016/j.molstruc.2021.131190.

#### **Publisher's Note & Disclaimer**

The statements, opinions, and data presented in this publication are solely those of the individual author(s) and contributor(s) and do not necessarily reflect the views of the publisher and/or the editor(s). The publisher and/or the editor(s) disclaim any responsibility for the accuracy, completeness, or reliability of the content. Neither the publisher nor the editor(s) assume any legal liability for any errors, omissions, or consequences arising from the use of the information presented in this publication. Furthermore, the publisher and/or the editor(s) disclaim any liability for any injury, damage, or loss to persons or property that may result from the use of any ideas, methods, instructions, or products mentioned in the content. Readers are encouraged to independently verify any information before relying on it, and the publisher assumes no responsibility for any consequences arising from the use of materials contained in this publication.